Available online at www.sciencedirect.com

ScienceDirect

Ceramics International 40 (2014) 4065–4069

CERAMICS INTERNATIONAL

www.elsevier.com/locate/ceramint

Synthesis and processing of spinel powders for transparent ceramics

M. Suarez[a,b,*], V. Rocha[a,b], A. Fernandez[a,b], J.L. Menendez[b], R. Torrecillas[b]

[a]*Fundación ITMA, Parque Tecnológico de Asturias, 33428 Llanera, Asturias, Spain*

[b]*Department of Nanostructured Materials, Centro de Investigación en Nanomateriales y Nanotecnología (CINN), Principado de Asturias – Consejo superior de Investigaciones Científicas (CSIC) – Universidad de Oviedo (UO), Parque Tecnológico de Asturias, 33428 Llanera, Asturias, Spain*

Received 12 June 2013; received in revised form 12 August 2013; accepted 12 August 2013
Available online 26 August 2013

Abstract

Spinel powders have been synthesized by chemical coprecipitation using two different precursors, nitrates and chlorides, and by an oxides mixture route. It has been shown that depending on the precursors used and the synthesis conditions pure spinel nanopowder can be obtained at different temperatures and with different levels of agglomeration. According to TEM results, the chloride route allows obtaining pure and deagglomerated spinel powders after calcination at 800 °C with a submicrometer particle size. Sintered lyophilized powders obtained by a chloride route allow achieving materials with in-line transmittances close to 46% at 540 nm and 83% in the infrared range.

Keywords: A. Sintering; C. Optical properties; D. Spinels

1. Introduction

Magnesium aluminate spinel ($MgAl_2O_4$) has received a great deal of attention as a technological important material due to its attractive properties such as high melting point (2135 °C), high mechanical strength at elevated temperatures, high hardness (16 GPa), high chemical inertness, relatively low density (3.58 g/cm^3) and good thermal shock resistance [1,2]. Furthermore, transparent magnesium aluminate spinel ($MgAl_2O_4$) ceramics have been considered as an important optical material due to its good mechanical properties and an excellent optical transmission from 0.2 to 5.5 μm, making it useful for a wide range of optical applications, including armor window strike-faces and protective windows for sensors, windows for barcode reader, pressure vessel, high index optics for ultraviolet microlithography, etc. [3–5].

Over the last decades, a variety of techniques [6–10] have been used to prepare $MgAl_2O_4$ spinel. However, for all the synthesis routes cited above the formation of coarse agglomerates during the drying process is a common problem that reduces sinterability and homogeneity of the microstructure in the formed product. Successful sintering of spinel ceramics has been demonstrated only with fine deagglomerated powders presenting chemical and phase purity and, very importantly, a narrow particle size distribution. In this sense, Tsukuma [11] sintered to transparency high purity TSP-15 powders produced by Taimei Chemical Industry with an average grain size (d_{50}) of 0.15 μm. Goldstein et al. [12] also prepared 2 mm thick transparent spinel disks at low temperature by using $MgAl_2O_4$ powder from Nanocerox, prepared by spray flame pyrolysis with a specific surface area of 30 m^2/g. In this case, it was also shown that a post hot isostatic press step improved the degree of transparency of the disks. Also, Krell et al. [13] produced dense spinel with a high transmittance in the visible range, starting with 55 nm spinel powders by carefully designing the sintering cycle, minimizing the grain growth to 300 nm without doping additives. Alternatively, fine powders doped with sintering aids, such as B_2O_3 [6], CaO [14], and LiF [15], were prepared to enhance the sinterability. However, second phases with a refractive index different from that of the matrix induce light scattering, reducing transmittance.

In this work, spinel particles are synthesized following two different routes: oxides mixture and reverse-strike coprecipitation and three different precursors: chlorides, nitrates and

*Corresponding author at: Fundación ITMA, Parque Tecnológico de Asturias, 33428 Llanera, Asturias, Spain. Tel.: +34 985 98 00 58; fax: +34 985 26 55 74.
E-mail address: msuarez@itma.es (M. Suarez).

0272-8842/$ - see front matter © 2013 Elsevier Ltd and Techna Group S.r.l. All rights reserved.
http://dx.doi.org/10.1016/j.ceramint.2013.08.060

oxides. It is shown how an adequate selection of the synthesis route and the processing conditions allows obtaining transparent spinel ceramics.

2. Experimental procedure

$MgAl_2O_4$ powders prepared by reverse-strike coprecipitation were synthesized using different precursors, magnesium and aluminum nitrates ($Mg(NO_3)_2 \cdot 9H_2O$ (ABCR) and $Al(NO_3)_3 \cdot 6H_2O$ (ABCR), respectively, and magnesium and aluminum chlorides ($MgCl_2 \cdot 6H_2O$ (Panreac) and $AlCl_3 \cdot 6H_2O$ (Fluka), respectively. Magnesium and aluminum nitrates or magnesium and aluminum chlorides were mixed with a 1:2 molar ratio, respectively. The pH value was kept constant at 10 ± 0.5 by adding ammonium hydroxide solution (Sigma-Aldrich, 28.0–30.0% in water) owing to the fact that is critical for the control of the chemical homogeneity within the particles. After 24 h of aging, a gelatinous precipitate was obtained. The amorphous gel was placed on a plate in a lyophilizer (CryoDos, Telstar) under vacuum (0.1 mbar) and held to -50 °C in order to remove the water by sublimation of the frozen gel. All powders were burnt at different temperatures in order to achieve a crystalline material. The raw materials in the oxides mixture, MgO (Merk) with an average particle size of around 1.6 μm and Al_2O_3 (Taimei, TM-DAR) with an average particle size of around 0.16 μm, were mixed in propanol with alumina balls for 1 h using an attrition mill. The powders were thermally calcined in air between 800 and 1200 °C for 2 h to obtain pure spinel. After the heating treatment the powders were ground in a ball mill and subsequently sieved through a mesh < 63 μm.

Thermogravimetric (TG) and differential temperature analysis (DTA) for the three products (TGA/DSC Star System, Mettler Toledo) were carried out under air atmosphere at a heating rate of 5 °C/min up to 1400 °C. The phase transitions of the heat-treated samples as a function of the temperature were followed by X-ray diffraction (Jobin Yvon, HORIBA) to determine the crystalline phases of the burnt powders. The particle size and the morphology of the Spinel nanopowders were investigated by TEM (2000FX, JEOL). The BET surface area of the samples was carried out under nitrogen atmosphere at 77 K (TriStar II 3020 V1.03, Micromeritics). Sintering was performed in a spark plasma sintering (SPS) apparatus (HPD 25/1, FCT) under low vacuum (10^{-1} mbar). Crystalline powders were placed into a graphite die with an inner diameter of 20 mm and sintered at the best temperature for each system for 3 min under an applied pressure of 50 MPa and a heating rate of 100 and 50 °C/min. The transmission spectrum was recorded on VIS (AvaSpec-2048, Avantes) and IR (IR-560, Nicolet Magna) equipments.

3. Results and discussion

The TG–DTA curve corresponding to nitrate precursors (Fig. 1(a)) shows four clear mass losses. The first one is a broad 16% weight loss over the temperature range 30–160 °C associated to an endothermic peak corresponding to the dehydration of adsorbed water in the powders. The second mass loss of 38%

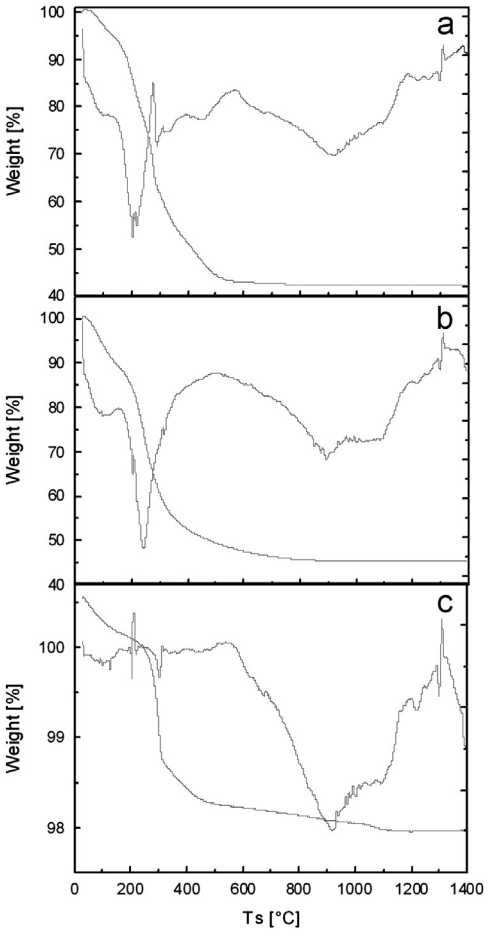

Fig. 1. TG/DTA plot of amorphous spinel powder for the nitrates (a), chlorides (b) and oxide (c) routes.

takes place between 160 and 285 °C that could be related to the intermolecular water. The third mass loss, between 285 and 389 °C, corresponds to the dehydroxylation of the mixed hydroxides to oxides. Finally the fourth mass loss, associated to an exothermic peak between 388 and 515 °C, could be attributed to the evaporation of NH_4NO_3 which appears during the synthesis as a by-product. The sharp exothermic peak between 1100 and 1200 °C is due to the crystallization of spinel.

Fig. 1(b) shows the TG curve corresponding to the chlorides route with a total weight loss about 55%. In this thermogram, an endothermic peak in the 40–150 °C with a mass loss of about 11% appears which may be associated to the vaporization of physically bound absorbed water. In the temperature region 150–450 °C, an endothermic peak appears that could be associated to the dehydroxylation of the mixed hydroxides to oxides. Finally the exothermic peak between 900 and 1200 °C is attributed to powders crystallization. According to the results the synthesis of spinel by chloride route requires a lower temperature to achieve a crystalline phase.

There is no sharp peak observed in the TG curve corresponding to the oxides mixture (Fig. 1(c)); just a broad exothermic peak starting at approximately 1000 °C and having a maximum at 1400 °C. Also, a minor weight loss (3%) is observed through all the temperature range studied.

These differences in the TG–DTA graphs suggest different behaviors in the synthesis of spinel and, therefore, different possibilities of tailoring the microstructure of the powders.

The structural characterization of the calcined samples has been done by X-ray diffraction (Fig. 2). Fig. 2(a) and b shows the X-ray diffraction for spinel synthesized by chloride and nitrate routes, respectively. According to these results, crystalline spinel is formed at 800 °C with well-defined peaks in the appropriate intensity relationships. A very different behavior is observed in Fig. 2(c), corresponding to X-ray diffraction pattern of burnt powders from oxide mixture. Below 1200 °C peaks other than those of spinel are observed. These peaks belong to a mixture of spinel and periclase phases, being necessary temperatures higher than 1200 °C to achieve a pure spinel structure for this synthesis route.

Specific surface area analyses have been performed on the three powders obtained. Powders produced by the oxides and nitrates routes show lower specific surface areas (15 and 18 m^2/g, respectively) than those produced following the chlorides route (41 m^2/g). This is an indication of a smaller grain size in the powders obtained in the chlorides route. The TEM images of the spinel powders prepared by the different routes and calcined at 1200 °C are shown in Fig. 3. According to the images nitrate and chloride routes (Fig. 3(a) and (b)) allow obtaining spinel powders with small grain size, around 20 nm. However, in case of nitrate route the powders show the presence of large agglomerated compared to the chlorides route. On the other hand, Fig. 3(c) belongs to powder synthesized by oxide mixture

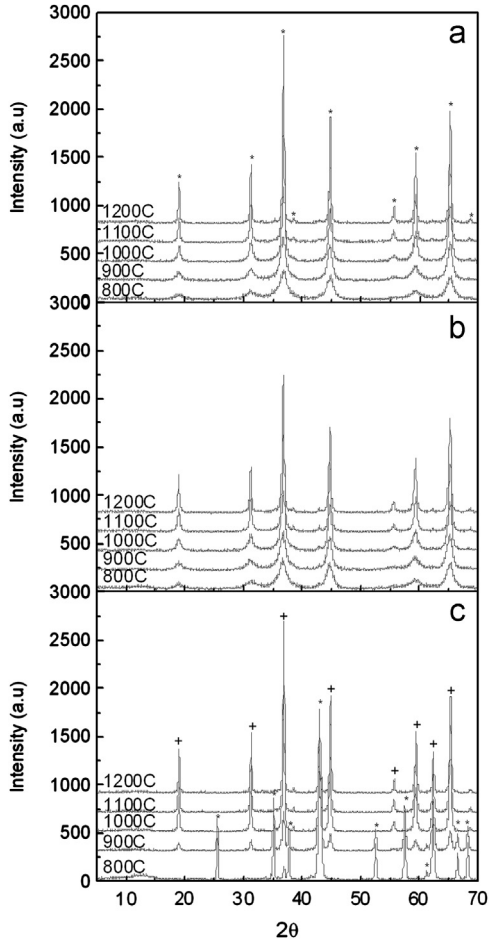

Fig. 2. X-ray diffractogram of powders calcined at temperatures between 800 and 1200 °C for the nitrates (a), chlorides (b) and oxides routes (c).

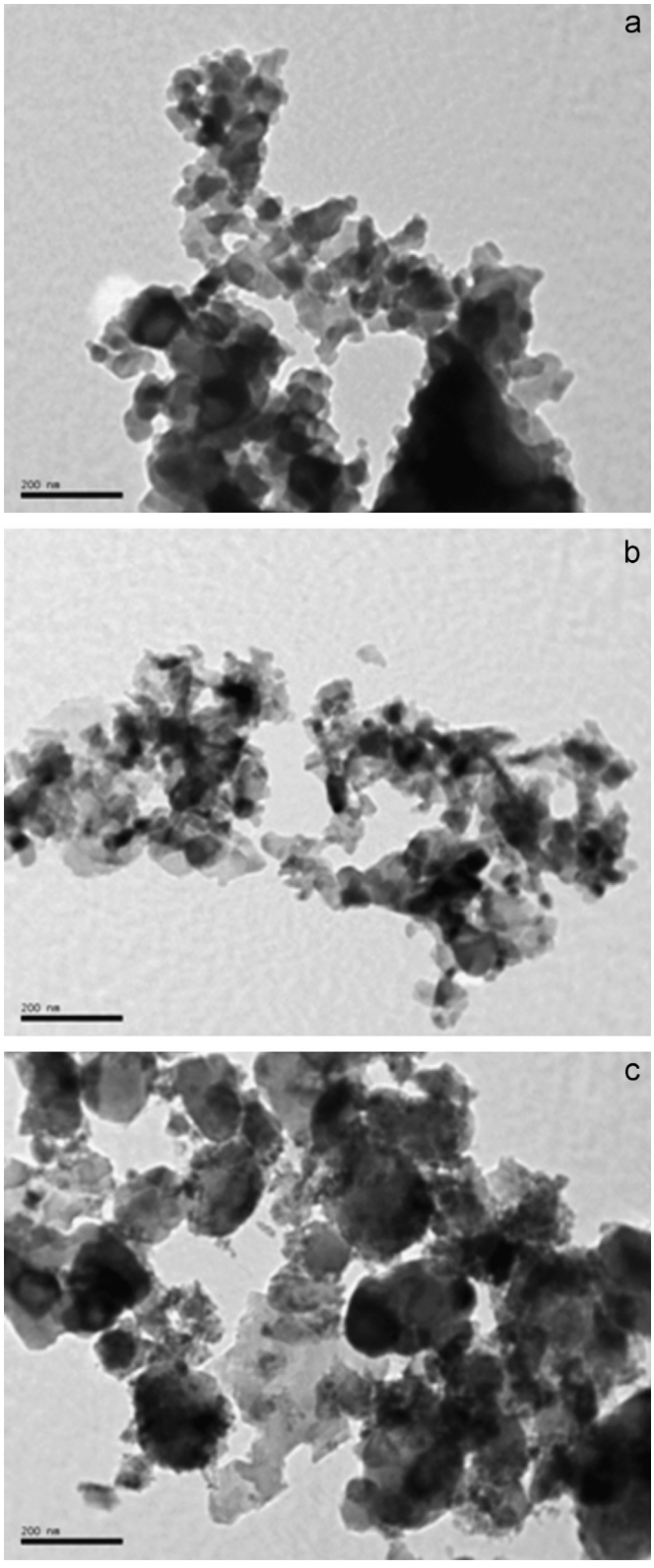

Fig. 3. TEM images of crystalline spinel powders prepared from (a) nitrates, (b) chlorides and (c) oxide mixture.

route and shows the presence of large agglomerates with an average particle size much larger than in the chloride and nitrate routes. The presence of these large agglomerates in case of oxide mixture powders has a negative impact on the forming behavior leading to cracks in the green body, as shown in Fig. 4 where three cracks are observed. The presence of these cracks in the green body affects the sintering behavior and the presence of pores and, therefore, the transmittance of the material. By comparing the morphology and the agglomeration level in the different synthesis routes, it can be concluded that chloride route is the best synthesis route to obtain powder free of agglomeration and with a homogeneous distribution of grain sizes.

In order to determine the sintering conditions, a dilatometric analysis was performed in the Spark Plasma apparatus up to 1600 °C for each powder. An example of the linear shrinkage curve and its derivative are shown in Fig. 5.

It can be seen that the material starts shrinking at 1100 °C approximately and the final sintering temperature is 1550 °C. The maximum speed is reached at 1300 °C. It is well-known that the lower dislocation density and the best in-line transmittance can be achieved by the higher superplastic deformation. According to Zhao et al. [16], a two-step pressure profile helps to decrease the dislocation density linked with the fast densification process in SPS and achieve better optical properties. For this reason, the better temperature for each powder was selected from the dilatometric analysis. During the cycle, two values of pressure, 5 and 16 kN, were applied and the heating rate was 50 and 100 °C/min.

Then, the real in-line transmittance (RIT) in the infrared and visible ranges for chloride, nitrate and oxide spinel powders was measured and it is shown in Fig. 6. The in-line transmittance of the sample was measured and then normalized to a thickness of 1 mm according to the following equation:

$$T = (1-R_s)\left\{T_{measured}/(1-R_s)\right\}^{t/d} \quad (1)$$

where, T is normalized transmittance, $R_s=(n-1)^2/(n^2+1)$; n is the refractive index, t is 1 mm, d is the actual thickness of the sample.

The RIT curves for each sintered sample are shown in Fig. 6. According to the results the highest transmittance is achieved with the spinel synthesized by chloride route, being of 83% in the infrared region and 46% at 540 nm. Although worse than the best transmittance results published in the literature [11–13], these values are comparable to the in-line transmittance reported previously in the case of spark plasma sintered spinel [17] and better than those reported in Ref. [18] when LiF was used as sintering aid by HIP technique. The inset in Fig. 6 shows that the samples are gray. It must be considered that in spark plasma sintering the ceramic powders are in close contact with the graphite molds and there is often some diffusion of carbon from the molds to the ceramic powders, which has also been observed by other groups [19–21] during SPS of spinel powders. This contributes to a blackening of the samples and, therefore, to lower transmittance values.

In order to analyze the RIT spectra, a model based on that given by Apetz and Van Bruggen [22] was developed. According to

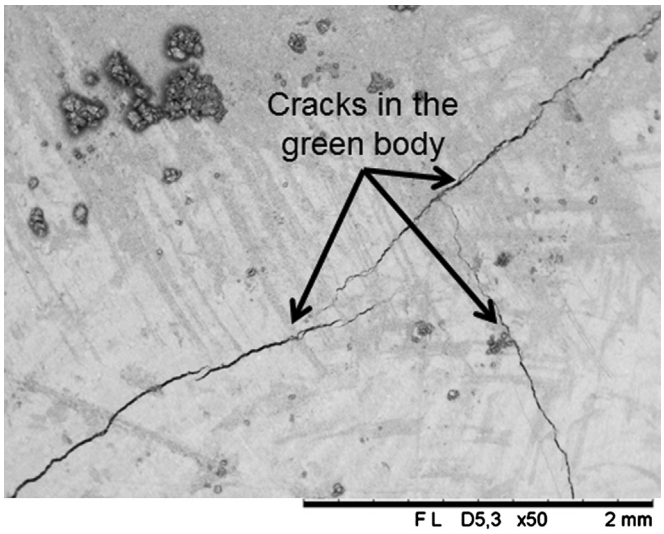

Fig. 4. SEM micrograph of a green body of spinel prepared from the oxides mixture showing three cracks after pressing process.

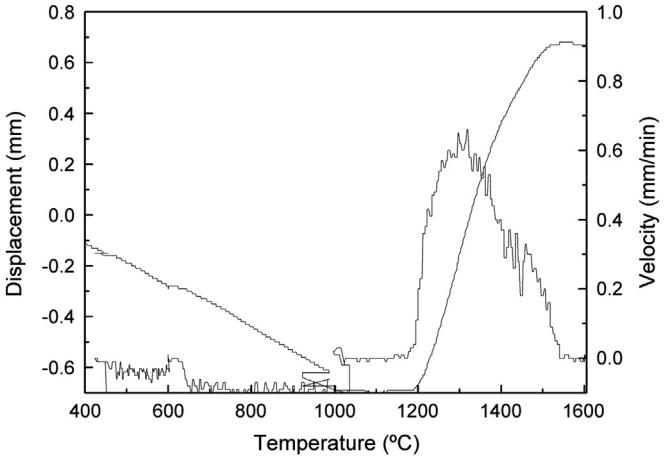

Fig. 5. Dilatometric linear shrinkage and velocity curve of spinel powders sintered at 1600 °C for 1 min with a 100 °C/min heating rate and a pressure of 5 kN.

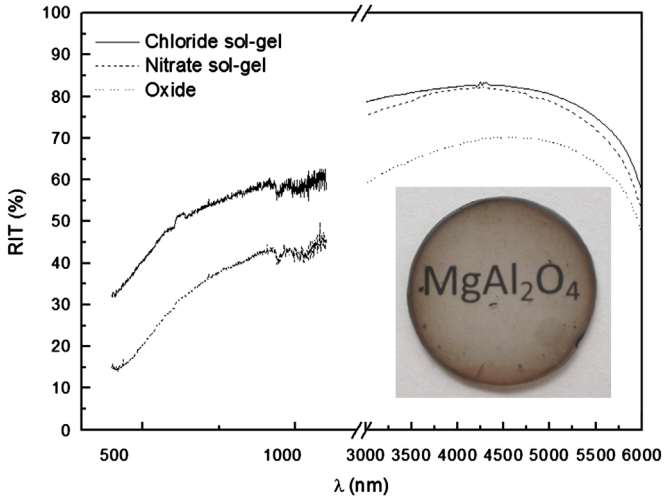

Fig. 6. Real in-line transmittance (RIT) curve for spinel synthesized by chloride (solid line), nitrate (dashed line) and oxide (dotted line) route. A picture of a spark plasma sintered spinel disk, obtained from the chloride route is shown in the inset.

Table 1
Pore size and porosity for the sintered samples.

Sample	Porosity (%)
Chloride sol–gel spinel	0.06
Nitrate sol–gel spinel	0.1
Oxide spinel	1.5

these authors, the RIT decays exponentially with the thickness of the sample. Assuming a constant pore size of 10 nm for the different samples, an idea can be obtained about the evolution of the total porosity in the different sintered materials (Table 1). Under this assumption, it is shown that the porosity of sample prepared by oxides route is an order of magnitude larger than in the nitrates and chlorides routes. It is very likely that both the average pore size and the total porosity are larger in this sample.

4. Conclusions

Oxides mixture and sol–gel with chlorides and nitrates as precursors have been used and compared in the synthesis of pure spinel powders. The chloride route allows obtaining single phase crystalline powders at lower temperatures (800 °C) with a submicrometer particle size. Spark plasma sintering of lyophilized powders obtained by a chloride route allow achieving materials with in-line transmittances close to 46% at 540 nm and 83% in the infrared range. Therefore, by a careful control of the synthesis, processing and sintering conditions, powders with high transmittance values can be obtained.

Acknowledgments

The authors acknowledge the Asturias Government for funding this work through Project PC010-45.

References

[1] J.-G. Li, T. Ikegami, J.-H. Lee, T. Mori, Y. Yajima, A wet-chemical process yielding reactive magnesium aluminate spinel ($MgAl_2O_4$) powder, Ceramics International 27 (2011) 481–489.
[2] N.M. Khalil, M.B. Hassana, E.M.M. Ewais, F.A. Saleha, Sintering, mechanical and refractory properties of MA spinel prepared via co-precipitation and sol–gel techniques, Journal of Alloys and Compounds 496 (2010) 600–607.
[3] A. Krell, T. Hutzler, J. Klimke, Transparent ceramics for structural applications. Part 2: fields of applications, Berichte der DKG 84 (2007) E50–E55.
[4] E. Strassburger, Ballistic testing of transparent armor ceramics, in: Proceedings of ECerS X, 2007, pp. 2257–2262.
[5] I. Reimanis, H.J. Kleebe, A review on the sintering and microstructure development of transparent spinel ($MgAl_2O_4$), Journal of the American Ceramic Society 92 (2009) 1472–1480.
[6] C. Pacurariu, I. Lazau, Z. Ecsedi, R. Lazau, P. Barvinschi, G. Marginean, New synthesis methods of $MgAl_2O_4$ spinel, Journal of the European Ceramic Society 27 (2007) 707–710.
[7] H. Reveron, D. Gutierrez-Campos, R.M. Rodrıguez, J.C. Bonassin, Chemical synthesis and thermal evolution of $MgAl_2O_4$ spinel precursor prepared from industrial gibbsite and magnesia powder, Materials Letters 56 (2002) 97–101.
[8] I. Ganesh, B. Srinivas, R. Johnson, B.P. Saha, Y.R. Mahajan, Microwave assisted solid state reaction synthesis of $MgAl_2O_4$ spinel powders, Journal of the European Ceramic Society 24 (2004) 201–207.
[9] V.K. Singh, R.K. Sinha, Low temperature synthesis of spine1 ($MgA1_20_4$), Materials Letters 3 (1997) 28l–285.
[10] C.R. Vestal, Z.J. Zhang, Normal micelle synthesis and characterization of $MgAl_2O_4$ spinel nanoparticles, Journal of Solid State Chemistry 175 (2003) 59–62.
[11] K. Tsukuma, Transparent $MgAl_2O_4$ spinel ceramics produced by HIP post-sintering, Journal of the Ceramic Society of Japan 114 (2006) 802–806.
[12] A. Goldstein, A. Goldenberg, M. Hefetz, Transparent polycrystalline $MgAl_2O_4$ spinel with submicron grains, by low temperature sintering, Journal of the Ceramic Society of Japan 117 (2009) 1281–1283.
[13] A. Krell, T. Hutzler, J. Klimke, A. Potthoff, Fine-grained transparent spinel windows by the processing of different nanopowders, Journal of the American Ceramic Society 93 (2010) 2656–2666.
[14] R.J. Bratton, Translucent sintered $MgAl_2O_4$, Journal of the American Ceramic Society 57 (1974) 283–286.
[15] K. Morita, B.N. Kim, K. Hiraga, H. Yoshida, Fabrication of transparent $MgAl_2O_4$ spinel polycrystal by spark plasma sintering processing, Scripta Materialia 58 (2008) 1114–1117.
[16] C. Wang, Z. Zhao, Transparent $MgAl_2O_4$ ceramic produced by spark plasma sintering, Scripta Materialia 61 (2009) 193–196.
[17] K. Morita, B.-N. Kin, K. Hiraga, H. Yoshida, Fabrication of transparent $MgAl_2O_4$ spinel polycrystal by spark plasma sintering processing, Scripta Materialia 58 (2008) 1114–1117.
[18] I.E. Reimanis, H.-J. Kleebe, R.L. Cook, A. DiGiovanni, Transparent spinel fabricated from novel powders: synthesis, microstructure and optical properties, in: Proceedings of the Defense and Security Symposium, 2004.
[19] S. Meir, S. Kalabukhov, N. Froumin, M.P. Dariel, N. Frage, Synthesis and densification of transparent magnesium aluminate spinel by SPS processing, Journal of the American Ceramic Society 92 (2009) 358–364.
[20] G. Bernard-Granger, N. Benameur, C. Guizard, M. Nygren, Influence of graphite contamination on the optical properties of transparent spinel obtained by spark plasma sintering, Scripta Materialia 60 (2009) 164–167.
[21] A. Goldstein, Correlation between $MgAl_2O_4$-spinel structure, processing factors and functional properties of transparent parts, Journal of the European Ceramic Society 32 (2012) 2869–2886.
[22] R. Apetz, M.P.B. Van Bruggen, Transparent alumina: a light-scattering model, Journal of the American Ceramic Society 86 (2003) 480–486.